J Mater Sci (2011) 46:422–428
DOI 10.1007/s10853-010-4882-9

Polyethylene/synthetic boehmite alumina nanocomposites: structure, mechanical, and perforation impact properties

V. M. Khumalo · J. Karger-Kocsis · R. Thomann

Received: 14 June 2010 / Accepted: 28 August 2010 / Published online: 11 September 2010

Abstract Synthetic boehmite alumina (BA) has been incorporated up to 8 wt% in high-density polyethylene (HDPE) and low-density polyethylene (LDPE) by melt compounding. The primary nominal particle sizes of the two BA grades used were 40 and 74 nm, respectively. The dispersion of the BA in PE matrices was investigated by scanning and transmission electron microscopy techniques (SEM and TEM). Specimens of the PE/BA nanocomposites were subjected to dynamic-mechanical thermal analysis (DMTA), static tensile and instrumented falling weight impact (IFWI) tests. It was established that BA was nanoscale dispersed in both HDPE and LDPE. According to DMTA, BA worked as reinforcing filler. This was confirmed in static mechanical tests, too. BA grades and contents influenced the static tensile and dynamic IFWI behaviors of the PE/BA nanocomposites differently. Surprisingly, BA incorporation enhanced the ductility (elongations at yield and break) of HDPE in contrast to LDPE. Unlike HDPE/BA nanocomposites, the perforation impact resistance of the LDPE/BA systems was reduced with increasing BA content at both ambient temperature and $T = -30$ °C. The lesser the reduction the higher the primary particle size of the BA was.

V. M. Khumalo · J. Karger-Kocsis
Polymer Technology, Faculty of Mechanical Engineering and Built Environment, Tshwane University of Technology, Pretoria 0001, Republic of South Africa

J. Karger-Kocsis (✉)
Polymer Engineering, Faculty of Mechanical Engineering, Budapest University of Technology and Economics, 1111 Budapest, Hungary
e-mail: karger@pt.bme.hu

R. Thomann
Institut für Makromolekulare Chemie und Freiburger Materialforschungszentrum, Albert-Ludwigs-Universität Freiburg, Stefan-Meier-Str. 31, 79104 Freiburg, Germany

Introduction

A large body of research and development works is focused nowadays on thermoplastic nanocomposites exhibiting improved and even novel properties. Most of the related studies concentrated on the structural performance of nanocomposites, and tried to deduce relationships between their structure and mechanical properties. Many of the potential nanofillers are polar substances (silica, layered silicates, metal oxides, and metal salts etc.) which can be poorly dispersed in apolar thermoplastics, such as polyethylenes (PEs). To support the dispersion of nanofillers, various strategies are followed. Nanofillers can be generated in situ (e.g. via sol–gel chemistry), their incorporation may occur in situ during polymer synthesis, they can be dispersed through solutions techniques and mixing in the melt, as well. Melt mixing of nanofillers in PEs is strongly favored as the properties of the nanocomposites can be easily tailored by their formulations. In addition, melt compounding in small quantities may still be economic by contrast to in situ polymerization. However, in order to achieve the necessary dispersion of nanofillers in melt blending, they should be surface modified and/or additional polymeric compatibilizer should be introduced. This is well documented in the literature (e.g. [1, 2]). For example, to improve the mechanical properties of PE/silica compounds the silica surface is usually coupled by silanes [3]. To produce PE/clay nanocomposites apart from using organophilic-modified clay (organoclay), also suitable compatibilizers (maleinated PE, copolymers composed of ethylene and polar comonomers) are introduced (e.g. [1, 2, 4]). Needless to emphasize that the

surface modification of the nanofillers and use of compatibilizers enhance the production costs of the related compounds. To overcome this problem, researchers try to avoid both the surface modification and compatibilization. Instead of organoclay, pristine clay can also be dispersed in thermoplastics via water-mediated melt compounding processes whereby the water swellability of clay is exploited (e.g. [5, 6]).

Interesting nanofillers for polyolefins which meet the above requirements (i.e. good dispersibility without surface treatment and couplants) are synthetic alumina (Al_2O_3) (e.g. [7]) and boehmite alumina (BA). BA with the chemical composition AlO(OH) can be produced in particulates with different aspect ratio. Their primary particle size is in the range of tens of nanometers. PE/BA nanocomposites were already produced by in situ polymerization [8, 9]. It was also shown that BA agglomerates can be broken up during melt compounding [10]. As BA is water dispersible it can be incorporated in suitable thermoplastics through water-mediated melt compounding as demonstrated recently [5, 11, 12]. Only few works addressed the effects of BA in PE-based systems [8, 9, 13]. Recent results demonstrating that BA incorporation strongly improved the resistance of PEs to thermooxidative degradation without affecting their melt viscosity [13] necessitate, however, further in depth studies on PE/BA nanocomposites. It is especially of great interest to check how the BA dispersion affects the mechanical performance of PE/BA nanocomposites to which the present work was dedicated. In order to get a deeper understanding on the structure–property relationships in the related nanocomposites, two BA grades and two PE types viz. high-density polyethylene (HDPE) and low-density polyethylene (LDPE) were used in this study. The platelet-shaped low aspect ratio BA was not surface-modified and its content in the PEs was varied between 0 and 8 wt%.

Experimental

Materials

Disperal® 40 and Disperal® 80 grades of Sasol GmbH (Hamburg, Germany) were used as BA nanofillers. Their nominal primary crystallite sizes are 40 and 74 nm, respectively.

LDPE grade LT388 (melt flow index at 190 °C/2.16 kg: 10 dg/min; density: 0.922 g/cm^3) from Sasol (Sasolburg, South Africa) and HDPE grade F 7740F2 (melt flow index at 190 °C/2.16 kg: 0.4 dg/min; density: 0.946 g/cm^3) from Safripol (Bryanston, South Africa) were used throughout this study.

Preparation of nanocomposites

Samples of HDPE and LDPE with BA were prepared via melt mixing using a Haake Rheomix OS internal mixer equipped with Polylab OS RheoDrive4 (Thermo Fischer Scientific, Karlsruhe, Germany). Mixing occurred for 8 min at 175 °C at 60 rpm for both PEs. Sheets of ca. 2 mm thickness have been produced by compression molding using a Carver press (Wabash, Indiana, USA). The temperature agreed with that of the mixing (=175 °C) and the pressure was set for 2 MPa. After ca. 5 min holding time, the press was cooled by water and the sheets demolded. For static tensile testing, the specimens were injection molded as described below.

The code of the materials followed next information about the PE type, content and type of the BA. Accordingly, HDPE4%BA80 represents a HDPE/BA nanocomposite containing Disperal® 80 in 4 wt%.

Testing

BA dispersion

The dispersion state of the BA particles in the PEs was studied by scanning electron microscopy (SEM) using a FEI Quanta 250 FEG device (FEI, Hillsboro, Oregon, USA). Specimens were cryomicrotomed with a Diatome diamond knife at $T = -120$ °C using a Leica EM UC6 ultramicrotome equipped with a cryo-chamber. The cryo-cut surfaces of the specimens were inspected in SEM (acceleration voltage 5 kV) without sputtering, using a high resolution vCD detector for backscattered electrons. The morphology of the samples was also studied in a transmission electron microscope (TEM). The TEM device (Zeiss LEO 912 Omega, Oberkochen, Germany) was working at an acceleration voltage of 120 kV. Thin specimens (thickness ca. 50 nm), prepared by cryocutting with the above ultramicrotome at $T = -120$ °C, were subjected to TEM investigations without any staining.

Dynamic-mechanical thermal analysis (DMTA)

DMTA measurements were performed on a Perkin Elmer (Waltham, MA, USA) DMA 8000 device under three point bending (3 PB) mode. DMA spectra were taken in the temperature range $T = -50$ °C (stabilized for 10 min) to $T = 140$ °C using a heat rate of 5 °C/min. During the tests, the frequency and displacement were constants, namely 1 Hz and 0.05 mm, respectively. The size of the specimens was: ca. 50 × ca. 6 × ca. 2 mm (length × width × thickness) and the span length in the 3 PB configuration was fixed at 35 mm.

Tensile mechanical behavior

For tensile testing, dumbbell specimens (tensile bar ASTM D638 type V) were produced by injection molding using a Haake Mini Jet 11 system (Thermo Fischer Scientific, Karlsruhe, Germany). The molding parameters set were: barrel: 175 °C, mold: 70 °C, injection pressure: 600 bar, cycle time: 120 s. Tensile tests were performed at RT using a small-scale tensile test machine (H10KT of Tinius Olsen, Redhill, Surrey, UK). The injection-molded dumbbell specimens were tested with a crosshead speed of 5 mm min^{-1} and the corresponding force–elongation curves registered. At least five specimens were tested for each material.

Instrumented falling weight impact (IFWI)

Sheets of ca. 2 mm thickness were compression molded using a Carver press (Wabash Indiana, USA). For molding of the sheets with 160 × 140 mm^2 surface, the following parameters were set: $T = 175$ °C, pressure = 2 MPa. After ca. 8 min holding time, the press was cooled by water and the sheets demolded. From the molded sheets, quadratic specimens (60 × 60 mm^2) were cut and subjected to IFWI. The specimens were perforated at RT and at $T = -30$ °C, respectively. At each temperature four specimens were tested using impact falling weight instrument (DAS 8000, Ceast, Pianezza, Italy). The experimental conditions were as followed: mass of falling dart with hemispherical tip: 23.620 kg, velocity: 4.43 m/s, height: 0.999 m (yielding incident impact energy of 231.40 J).

Results and discussion

BA dispersion

Figures 1 and 2 show SEM pictures taken from the cryocut surfaces of HDPE/BA and LDPE/BA nanocomposites with 4 wt% BA40. The SEM photos in Figs. 1 and 2 already indicate that the finely and rather uniformly dispersed BA particles are agglomerated though their particle agglomerate size is still in submicron scale. Moreover, a closer inspection of the high magnification SEM microphotographs suggests that the BA particles easily detach from the matrix (cutting of the specimens caused this kind of debonding phenomenon) and the crystallization of the PE is not influenced (the lamellar structure is similar close to the BA particle and in the bulk PE). In fact, we have shown in our companion article that the crystallinity of the PE matrices, measured by differential scanning calorimetry, was not affected by the presence of BA nanoparticles [13].

TEM pictures in Fig. 3 substantiate that the designation nanocomposite is correctly used. One can also recognize on the example of HDPE/BA80 that with increasing BA content no further agglomeration of the BA particles takes place (cf. Fig. 3b, c). The difference in the primary crystallite sizes of the BA grades is well perceptible by comparing the TEM pictures in Fig. 3a and b.

The above morphological results confirm that synthetic BAs can finely be dispersed in PEs even without using coupling agents and polymeric compatibilizers.

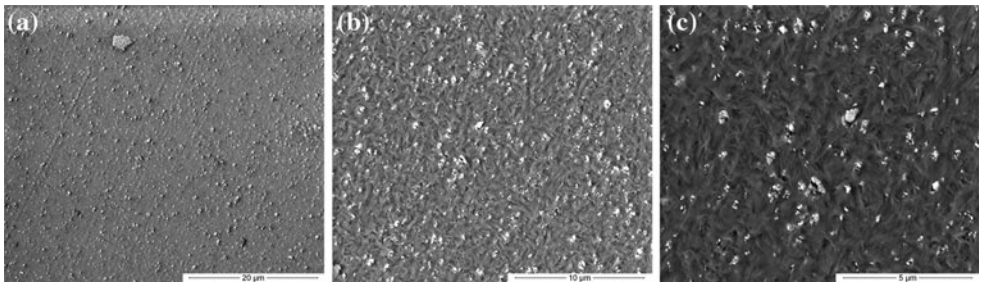

Fig. 1 SEM micrographs taken at different magnifications from the cryocut surfaces of HDPE4%BA40

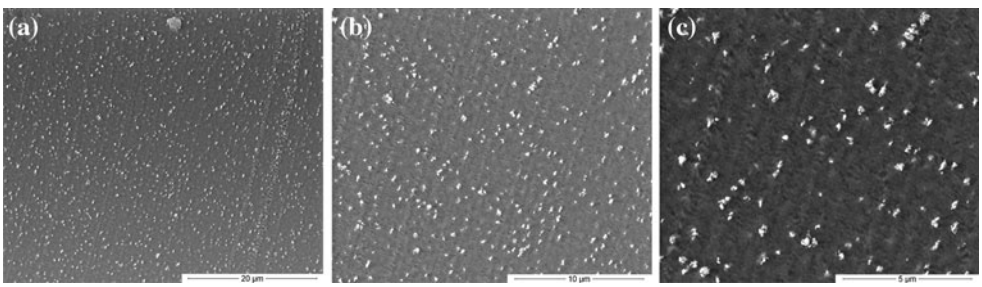

Fig. 2 SEM micrographs taken at different magnifications from the cryocut surfaces of LDPE4%BA40

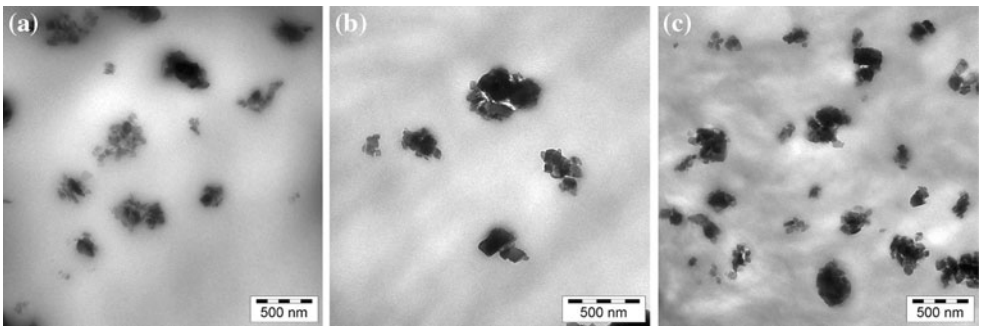

Fig. 3 Characteristic TEM pictures taken from HDPE4%BA40 (**a**), HDPE4%BA80 (**b**) and HDPE8%BA80 (**c**), respectively, at the same magnification

DMTA spectra

Figure 4a and b show the storage modulus (E'; stiffness) and mechanical loss factor (tan δ) as a function of temperature (T) for the HDPE and HDPE/BA nanocomposites containing 8 wt% BA. The stiffness of the HDPE/BA nanocomposites was higher than the reference HDPE in the whole temperature range studied. This is a clear indication for the reinforcing effect of the BA nanoparticles. On the other hand, the BA grade did not affect the E' of the nanocomposites. This was not the case at 4 wt% BA contents. The stiffness increment at 4 wt% BA40 was already the same as at 8 wt%. On the other hand, marginal effect on stiffness could be noticed for BA80 when added in 4 wt%. The alpha-relaxation transition at $T = 60$ °C became less resolved with increasing BA content (cf. Fig. 4b). This is in line with the expectation when considering the physical reason of the transition, viz. segmental motion in the amorphous phase in the vicinity of the PE crystal lamellae [14, 15]. As the latter is hampered by the nanofiller, the peak intensity of the alpha-relaxation is reduced. However, the position of this peak did not change which hints that the crystalline superstructure of the matrix remained the same. Recall that this was prophesied based on the SEM picture in Fig. 1c. The steep increase in tan δ prior to specimen melting occurs at higher temperature in the nanocomposites than in the HDPE reference sample. This, along with the improvement in E' in the whole temperature range, suggests that the heat distortion temperature of the HDPE is also enhanced by the BA nanofillers.

The DMTA spectra of LDPE/BA nanocomposites (cf. Fig. 5) differ from those of the HDPE/BA versions (cf. Fig. 4). The reinforcing effect of BA in LDPE is obvious based on the E' versus T trace. Moreover, BA40 works somewhat better than BA80 that should be ascribed to the smaller primary particle size and thus higher specific surface of the former compared to the latter BA grade (cf. Fig. 5a). In the tan δ versus T traces, two relaxation transitions can be resolved: the alpha at $T = 60$ and the beta one at $T = -20$ °C. Like HDPE/BA, the intensity of the alpha peak of LDPE was reduced in presence of BA. This is a manifestation of the reinforcing effect of BA. However, the position of this peak did not change with BA incorporation. This suggests no alteration in the crystalline supermolecular structure (already deduced based on the SEM picture in Fig. 2c) and a moderate reinforcing effect (no peak shift toward higher temperatures). This behavior is similar to what found for HDPE/BA. The beta-relaxation is linked with the molecular branching of the LDPE. As the branching is a material characteristic [14], the beta-peak should not be impaired by the BA nanofillers, which was established, indeed.

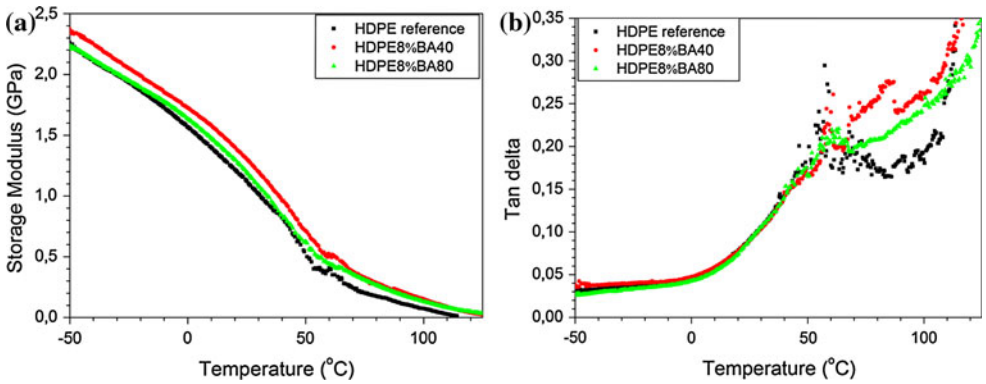

Fig. 4 E' versus T (**a**) and tan δ versus T traces (**b**) for HDPE and HDPE/BA (8 wt%) nanocomposites

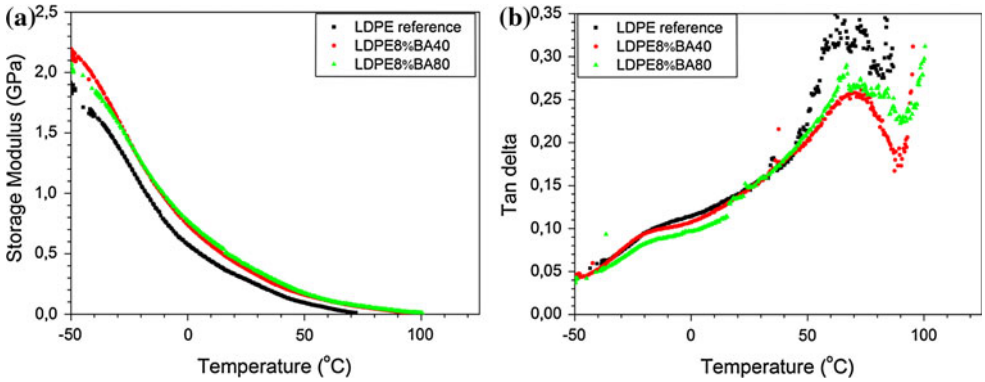

Fig. 5 E' versus T (**a**) and tan δ versus T traces (**b**) for LDPE and LDPE/BA (8 wt%) nanocomposites

Table 1 Static tensile mechanical characteristics of the PEs and PE/BA nanocomposites

Materials	Properties			
	Young's modulus [MPa]	Yield strength [MPa]	Elongation at yield [%]	Elongation at break [%]
HDPE reference	1280 ± 53	34.4 ± 3	12 ± 0.5	19 ± 2
HDPE4%BA40	1315 ± 62	31.3 ± 4	9 ± 0.9	40 ± 7
HDPE8%BA40	1326 ± 80	30.1 ± 2	10 ± 0.6	40 ± 11
HDPE4%BA80	1320 ± 64	29.8 ± 3	10 ± 0.7	43 ± 7
HDPE8%BA80	1339 ± 71	31.7 ± 4	9 ± 2	36 ± 9
LDPE reference	164 ± 15	14.7 ± 0.1	54 ± 6	88 ± 8
LDPE4%BA40	216 ± 22	14.2 ± 0.5	40 ± 4	81 ± 5
LDPE8%BA40	235 ± 18	13.9 ± 0.5	37 ± 3	78 ± 8
LDPE4%BA80	180 ± 15	14.0 ± 0.5	51 ± 6	90 ± 10
LDPE8%BA80	200 ± 15	14.0 ± 05	47 ± 1	81 ± 8

Tensile mechanical behavior

The static tensile mechanical properties are tabulated in Table 1. Accordingly, the Young's modulus (stiffness) of the PE/BA nanocomposites increased with BA content for both HDPE and LDPE. The effect of BA grade was marginal for HDPE, but pronounced for LDPE. BA40 acted as more efficient reinforcement in LDPE than BA80. The yield strength of HDPE was slightly reduced, the elongation at yield practically unaffected, and the elongation at break markedly enhanced (more than doubled) by BA incorporation. The latter can be explained by the following failure mode: particle debonding with massive voiding occurs first. This is followed by void coalescence associated with matrix fibrillation.

In case of LDPE, the Young's modulus was strongly enhanced, as mentioned above, and also influenced by the BA grade. On the other hand, the yield strength, elongation at yield, and elongation at break values were only slightly affected by the BA filler. It is noteworthy that the failure mode and sequence of LDPE/BA were similar to those of HDPE/BA though not affecting the gross yielding. The above results are of great practical relevance as the stiffness and heat distortion temperature (for the latter only indirect evidence was delivered) were improved without affecting ductility characteristics of the corresponding PE. To check whether or not the excellent ductility of PE/BA was kept under dynamic conditions, nanocomposite sheets were subjected to transverse perforation impact.

Instrumented falling weight impact (IFWI)

From the IFWI fractograms, the following parameters were read and computed: peak force (F_{peak}), energy absorbed until F_{peak} (E_{peak}), and total perforation impact energy (E_{total}). Since the thickness of the PE/BA nanocomposite sheets differed from one another (varied between 2.1 and 2.4 mm) the above parameters were normalized to the thickness of the specimens and the related specific values were considered, viz. F_{peak}/t, E_{peak}/t, and E_{total}/t, where "t" denotes the thickness. In addition, the ductility index (DI) was computed. DI indicates the ratio of the energy absorbed after the maximum (peak) load was reached. Traditionally, the energy absorbed until F_{peak} (i.e. E_{peak}) is considered as the energy required for crack initiation, whereas $E_{total} - E_{peak}$ represents the absorbed energy during crack propagation [16]. DI, defined by DI $= (E_{total} - E_{peak})/E_{total}$, and having a value between 0 (ideally brittle) and 1 (ideally

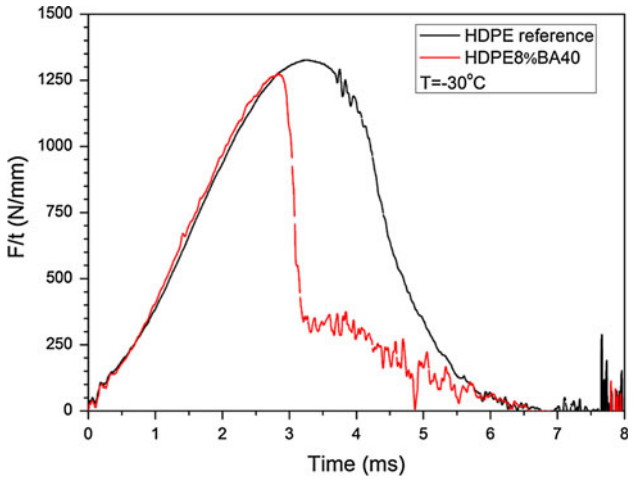

Fig. 6 Characteristic thickness-related force (F/t) versus time fractograms for HDPE and HDPE8%BA40, registered at $T = -30$ °C

ductile), provides information about the failure mode of the specimen. Figure 6 collates characteristic force–time traces of HDPE and HDPE8%BA40 registered at $T = -30$ °C. This selection was based on the IFWI results, summarized in Table 2, indicating that the perforation impact characteristics were not significantly affected by the BA nanoparticles. On the other hand, the fractograms in Fig. 6 already hint via the reduction in the surface below the normalized force versus time traces that BA incorporation "embrittled" the HDPE. In fact, E_{peak}/t, E_{total}/t, and DI all mostly decreased with increasing BA content—the related trend becomes clear when looking at the mean values summarized in Table 2.

Effects of BA grade and content turn more clearly when considering the results achieved on LDPE instead of HDPE. BA40, being a more efficient reinforcing filler than BA80 in LDPE, causes pronounced embrittlement, whereas the effect of BA80 on the IFWI parameters is marginal at both testing temperatures (cf. Fig. 7 and related results in Table 2).

It is interesting to note that with decreasing testing temperature, the IFWI parameters—except DI which is always reduced—become higher. This is due to the increased Young's modulus of the material which is not accompanied with substantial change in ductility characteristics as the lowest testing temperature (i.e. $T = -30$ °C) is still far beyond the glass transition (T_g, gamma-relaxation) of PE. Note that T_g is well below the lower threshold temperature set for the DMTA measurements.

Conclusion

This work was devoted to determine the effects of synthetic boehmite alumina (BA) on the morphology, DMTA, static

Table 2 IFWI characteristics of the PEs and PA/BA nanocomposites

Materials	F_{peak}/t (kN/mm) [RT]	E_{peak}/t (J/mm) [RT]	E_{total}/t (J/mm) [RT]	DI [RT]	F_{peak}/t (kN/mm) [−30 °C]	E_{peak}/t (J/mm) [−30 °C]	E_{total}/t (J/mm) [−30 °C]	DI [−30°]
HDPE reference	1.19	8.7	16.9	0.48	1.39	10.7	18.8	0.43
HDPE4%BA40	1.17	8.5	13.3	0.36	1.14	7.5	12.8	0.41
HDPE8%BA40	1.05	6.9	11.3	0.39	1.26	7.6	11.7	0.35
HDPE4%BA80	1.18	8.9	17.7	0.50	1.09	7.5	13.3	0.43
HDPE8%BA80	1.17	9.2	17.5	0.47	1.19	9.0	16.4	0.45
LDPE reference	0.87	6.2	12.9	0.52	1.09	6.7	15.2	0.56
LDPE4%BA40	0.86	6.7	9.9	0.32	1.17	10.3	13.6	0.26
LDPE8%BA40	0.73	4.4	6.1	0.27	0.67	2.1	2.2	0.05
LDPE4%BA80	0.83	6.2	10.3	0.40	1.12	8.3	14.0	0.41
LDPE8%BA80	0.80	6.3	9.9	0.36	1.14	8.8	13.8	0.36

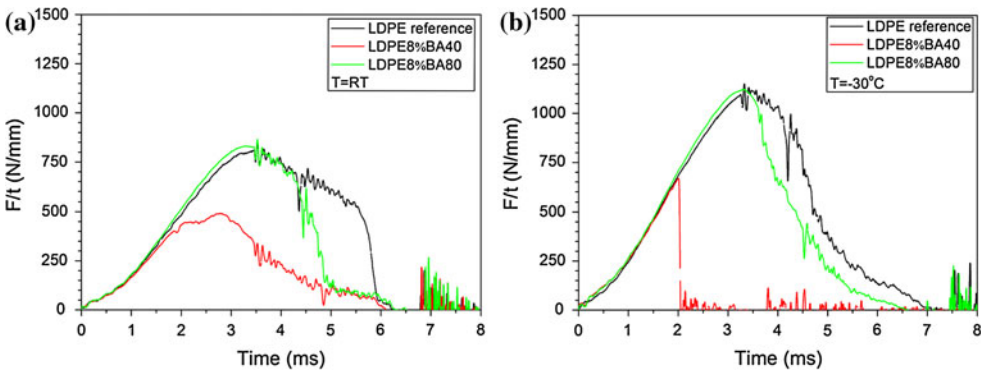

Fig. 7 Characteristic thickness-related force (F/t) versus time fractograms for LDPE, LDPE8%BA40, and LDPE8%BA80, registered at RT (**a**) and $T = -30$ °C (**b**), respectively

tensile, and dynamic perforation impact behaviors of polyethylenes (PEs). BA was incorporated, up to 8 wt%, in both HDPE and LDPE through melt compounding. It was established that BA was nanoscale and rather uniformly dispersed, though agglomerated, in the corresponding PEs. BA worked as reinforcement more efficiently in LDPE than in HDPE. This can be ascribed to the lower crystallinity of the LDPE compared to the HDPE. On the other hand, BA incorporation improved the ductility (tensile elongation data) of the HDPE by contrast to LDPE. The dynamic perforation impact (IFWI) behavior of HDPE/BA was less influenced by the BA type and amount at both testing temperatures (i.e. RT and −30 °C). On the contrary, the IFWI response of the LDPE/BA nanocomposites depended on the type and amount of BA. BA40 strongly reduced the IFWI characteristics compared to BA80, and when added in 8 wt% induced brittle fracture at $T = -30$ °C.

Acknowledgements This work was part of a collaboration project between Hungary and Republic of South Africa (RSA). The authors thank Prof. S. Sinha Ray (Nanocenter—Council for Scientific and Industrial Research, Pretoria, RSA) for preparation and testing facilities. The BA was kindly provided by Dr. O. Torno (Sasol GmbH, Hamburg, Germany).

References

1. Michler GH, Baltá-Calleja FJ (eds) (2005) Mechanical properties of polymers based on nanostructure and morphology. CRC Press, Boca Raton, FL, USA
2. Utracki LA (2004) Clay-containing polymeric nanocomposites. Rapra Technology, Shawbury, Shropshire, UK
3. Dorigato A, Pegoretti A, Penati A (2010) eXPRESS Polym Lett 4:115. doi:10.3144/expresspolymlett.2010.16
4. Karger-Kocsis J (2009) In: Karger-Kocsis J, Fakirov S (eds) Nano- and micro-mechanics of polymer blends and composites, chap 12. Hanser, Munich, p 425
5. Siengchin S, Karger-Kocsis J (2009) Compos Sci Technol 69:677. doi:10.1016/j.compscitech.2009.01.003
6. Siengchin S, Karger-Kocsis J, Apostolov AA, Thomann R (2007) J Appl Polym Sci 106:248. doi:10.1002/app.26474
7. Malucelli G, Palmero P, Ronchetti S, Delmastro A, Montanaro L (2010) Polym Int 59:1084. doi:10.1002/pi.2832
8. Halbach TS, Thomann Y, Mülhaupt R (2008) J Polym Sci Part A Polym Chem 46:2755. doi:10.1002/pola.22608
9. Halbach TS, Mülhaupt R (2008) Polymer 49:867. doi:10.1016/j.polymer.2007.12.007
10. Streller RC, Thomann R, Torno O, Mülhaupt R (2008) Macromol Mater Eng 293:218. doi:10.1002/mame.200700354
11. Siengchin S, Karger-Kocsis J (2010) Composites Part A Appl Sci Manuf 41:768. doi:10.1016/j.compositesa.2010.02.009
12. Siengchin S, Karger-Kocsis J, Thomann R (2007) J Appl Polym Sci 105:2963. doi:10.1002/app.26505
13. Khumalo VM, Karger-Kocsis J, Thomann R (2010) eXPRESS Polym Lett 4:264. doi:10.3144/expresspolymlett.2010.34
14. Molefi JA, Luyt AS, Krupa I (2010) J Mater Sci 45:82. doi:10.1007/s10853-009-3894-9
15. Popli R, Glotin M, Mandelkern L, Benson RS (1984) J Polym Sci Polym Phys Ed 22:407. doi:10.1002/pol.1984.180220306
16. Bucknall CB (1992) Plast Rubb Compos Process Appl 17:141